# Effective Mass and $g$ Factor of Four-Flux-Quanta Composite Fermions

A. S. Yeh,[1] H. L. Stormer,[2,3] D. C. Tsui,[1,4] L. N. Pfeiffer,[2] K. W. Baldwin,[2] and K. W. West[2]
[1]*Department of Physics, Princeton University, Princeton, New Jersey 08540*
[2]*Bell Labs, Lucent Technologies, Murray Hill, New Jersey 07974*
[3]*Department of Physics and Department of Applied Physics, Columbia University, New York, New York 10023*
[4]*Department of Electrical Engineering, Princeton University, Princeton, New Jersey 08540*
(Received 14 July 1998)

We investigate the properties of composite fermions with four attached flux quanta through tilted-field experiments near Landau level filling factor $\nu = 3/4$. The observed collapse of fractional quantum Hall gaps in the vicinity of this quarter-filling state can be comprehensively understood in terms of composite fermions with mass and spin. Remarkably, the effective mass and $g$ factor of these four-flux-quanta composite fermions around $\nu = 3/4$ are very similar to those of two-flux-quanta composite fermions around $\nu = 3/2$. [S0031-9007(98)08208-8]

PACS numbers: 71.10.Pm, 71.18.+y, 73.40.Hm

Our view of the fractional quantum Hall effect (FQHE) [1] has expanded considerably during the past several years. The composite fermion (CF) model [2,3] has provided an elegant and rather intuitive interpretation of the different sequences of FQHE states. It transforms the system of interacting electrons into an equivalent system of noninteracting fermions by the attachment of an even number $2m$ of magnetic flux quanta to each electron. The resulting particles are named CFs. At exact even denominator filling factors $\nu = 1/2m$, the attached flux and the external flux cancel exactly in the mean field approximation, and one arrives at a Fermi sea of CFs in a vanishing *effective* magnetic field. In other external magnetic fields, the cancellation is not exact; the CFs experience a nonzero effective magnetic field, and their orbital motion is quantized into CF Landau levels. The magnetic fields at which the $\nu = p/(2mp \pm 1)$ FQHE states are seen in experiment correspond precisely to those of the CF Landau gaps, and the FQHE can be viewed as an integral quantum Hall effect (IQHE) of such strange composite particles.

A large body of experimental work has amassed around filling factor $\nu = 1/2$ in support of the simplest of CFs, consisting of two flux quanta attached to each electron ($^2$CFs). Geometrical resonance experiments have demonstrated the existence of a well-defined Fermi wave vector [4]. In addition, activation energy and Shubnikov–de Haas measurements on the sequence of FQHE states $\nu = p/(2p \pm 1)$ converging on $\nu = 1/2$ determine an effective mass, which originates *solely* from electron-electron interactions [5].

Tilted-field experiments on $^2$CFs, performed mostly around $\nu = 3/2$, reveal repeated collapses of the surrounding FQHE gaps [6]. Today these features are comprehensively explained in terms of CFs carrying spin and $g$ factor [7]. As a function of tilt, crossing of spin-split CF Landau levels leads to vanishing energy gaps, whenever the CF Zeeman energy is a multiple of the CF Landau energy. For a given specimen all such coincidences can be understood in terms of an only slightly varying CF mass and $g$ factor. This is a remarkable fact, since the $g$ factor is strongly affected by exchange, which is expected to differ substantially between different FQHE states.

The bulk of the experimental and theoretical work investigates the properties of CFs with two attached flux quanta, i.e., $m = 1$. Very little is known about higher order CFs at $\nu = 1/2m$ $(m > 1)$, or at $\nu = i \pm 1/2m$, which are particle-hole conjugates of the former or reside in higher Landau levels. FQHE states associated with any such higher order CFs are much more fragile than the states around half filling and have considerably weaker energy gaps.

In this paper we investigate effective mass and $g$ factor of four-flux-quanta composite fermions, $^4$CFs, by performing angular and temperature dependent electrical transport experiments on the FQHE states at $\nu = (3p \pm 1)/(4p \pm 1)$ around filling factor $\nu = 3/4(= 1 - 1/4)$. As in the case of $\nu = 3/2$, all our experimental findings can be parametrized in terms of an effective mass, which is only density dependent and a practically constant $g$ factor. Most importantly, the parameters derived for $^4$CFs turn out to be very similar to those of $^2$CFs.

The four samples examined are high-mobility modulation-doped GaAs/AlGaAs heterostructures. They have electron densities of $n = (0.86, 1.13, 2.17,$ and $2.26) \times 10^{11}$ cm$^{-2}$ and mobilities of $\mu = (11, 6.8, 6.2,$ and $13) \times 10^6$ cm$^2$/V s, respectively. We refer to them by their density in $10^{11}$ cm$^{-2}$, i.e., sample 1.13 for the specimen of density $n = 1.13 \times 10^{11}$ cm$^{-2}$. The samples are cleaved into 5 mm $\times$ 5 mm squares, each of which has eight diffused indium contacts placed symmetrically around the perimeter. The experiments are performed in a top-loading dilution refrigerator with an *in situ* sample rotation stage.

Magnetoresistance data were taken around $\nu = 3/4$ for sample 0.86 at 71 different tilt angles between $\theta = 0°$

 0031-9007/99/82(3)/592(4)$15.00 

and 70° at temperature $T = 55$ mK, for sample 1.13 at 36 angles between $\theta = 0°$ to 61° at $T = 32$ mK, for sample 2.17 at 25 angles between $\theta = 0°$ and 51° at $T = 42$ mK, and for sample 2.26 at 44 angles between $\theta = 0°$ to 51° at $T = 41$ mK. Figure 1 contains an overview of the FQHE for sample 1.13 at ~40 mK.

In all samples, the FQHE minima at given filling factors show a complex angular dependence, successively weakening and strengthening with tilt angle (see inset of Fig. 1). In Fig. 2 we plot the amplitude at FQHE states $\nu = (3p \pm 1)/(4p \pm 1)$ as a function of the total external magnetic field, $B_{\rm tot} = B_\perp/\cos\theta$. In addition, for each maximum we check whether the FQHE state is actually resolved as a clear minimum in the original data, on *both* sides of the maximum in Fig. 2. Maxima with bold labels in Fig. 2 have these additional strong characteristics. Maxima with italic labels show a well-defined state only on one side of the peak in Fig. 2. Such occurrences at the edge of the range of $B_{\rm tot}$ may indicate a true maximum just beyond reach. Maxima with italic labels in the center of Fig. 2 may be the result of an underlying rising background.

The structure of Fig. 2 is similar to the one seen in the angular dependence experiment around $\nu = 3/2$ [7]. At this half filling, the complex behavior of the magnetoresistance is explained by a simple model in which CFs have a mass $m^*$ and a $g$ factor $g^*$. This leads to the simple energy level diagram seen in the inset of Fig. 2. For any given FQHE state, the CF Landau level splitting, $E_C$, remains fixed under tilt, whereas the Zeeman splitting, $E_Z$, increases linearly with $B_{\rm tot}$. This leads to level crossings and, hence, disappearances of energy gaps whenever $E_Z = jE_C$ or $g^*\mu_B B_{\rm tot} = j\hbar\omega_c = j\hbar eB_{\rm eff}/m^*$, for integral $j$.

In analogy to the $^2$CF behavior around $\nu = 3/2$, we regard the resistance maxima of Fig. 2 as resulting from the crossings of spin-split $^4$CF Landau levels. These FQHE states at $\nu = (3p \pm 1)/(4p \pm 1)$ are the IQHE states $p$ of $^4$CFs originating from $\nu = 3/4$. Their orbits are quantized into Landau levels by the effective magnetic field $B_{\rm eff} = -3(B_\perp - B_{\perp,\nu=3/4})$, where $B_{\perp,\nu=3/4}$ is the perpendicular field at $\nu = 3/4$, and their cyclotron energies are $E_C = \hbar eB_{\rm eff}(4\nu/3)^{0.5}/m^*_{\nu=3/4}$ [3]. The factor $(4\nu/3)^{0.5}$ establishes electron-hole symmetry. Since it varies only from 1.03 to 0.98 for the fractions of our experiment, we disregard it for the sake of simplicity. Therefore, coincidences occur when $B_{\rm tot}/B_{\rm eff} = 2j/g^*m^*$.

Guided by this relation, we plot in Fig. 3 $B_{\rm tot}$ vs $B_{\rm eff}$ for *all* observed resistance maxima in *all* our samples. The ordinate is proportional to the $^4$CF Zeeman splitting, and the abscissa is proportional to the $^4$CF cyclotron

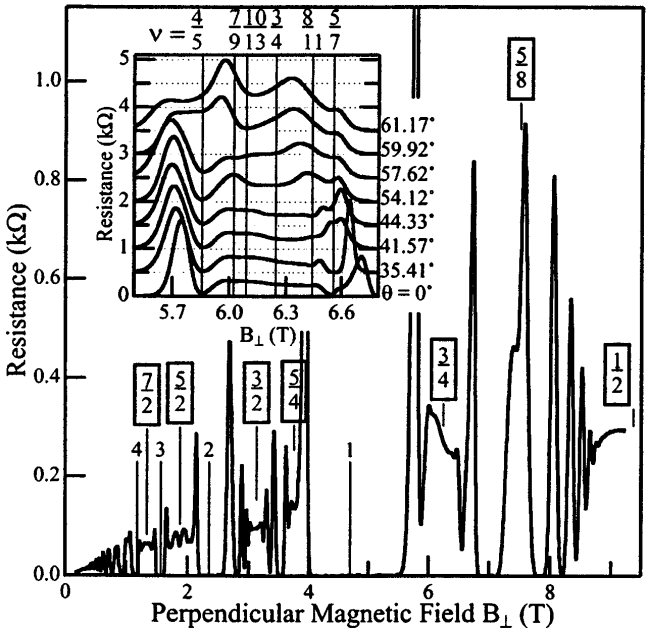


FIG. 1. Overview of the FQHE in sample 1.13 at $T \sim 40$ mK. The FQHE features around even-denominator filling factors $\nu$ (boxes) can be regarded as the magnetoresistance oscillations due to the formation of composite fermion Landau levels. The inset shows the magnetoresistance around $\nu = 3/4$ for the same sample at selected tilt angles. Traces are vertically offset by 500 ohms for clarity.

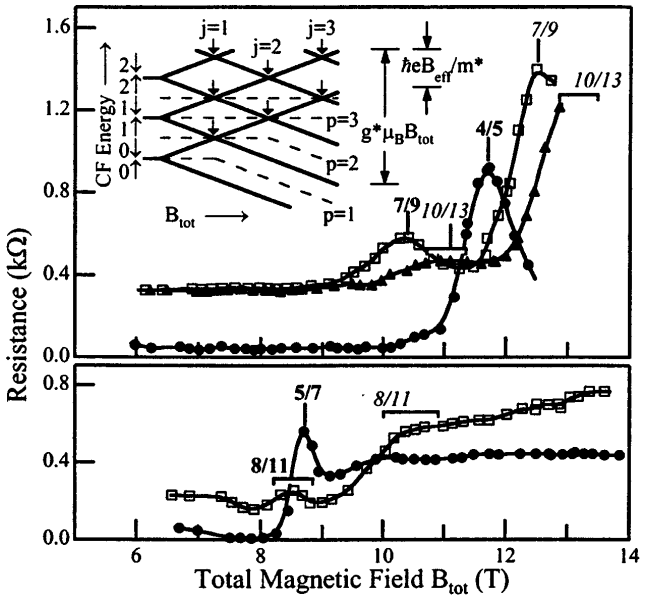


FIG. 2. Angular dependence of the magnetoresistance at FQHE states around $\nu = 3/4$. $B_{\rm tot} = B_\perp/\cos\theta$ is the total external magnetic field at tilt angle $\theta$. Maxima are indicated by vertical lines and brackets. The bold labels indicate maxima supported by stronger evidence, as described in the text. The inset shows a simple energy level diagram for CFs with spin (solid lines) for constant $B_\perp$ and increasing $B_{\rm tot}$. Level crossings occur when the CF Landau energy $\hbar eB_{\rm eff}/m^*$ is a multiple $j$ of the CF Zeeman energy $g^*\mu_B B_{\rm tot}$, as indicated by arrows. The Fermi levels for CF filling factor $p = 1$, 2, 3, and 4 are shown as dashed lines.

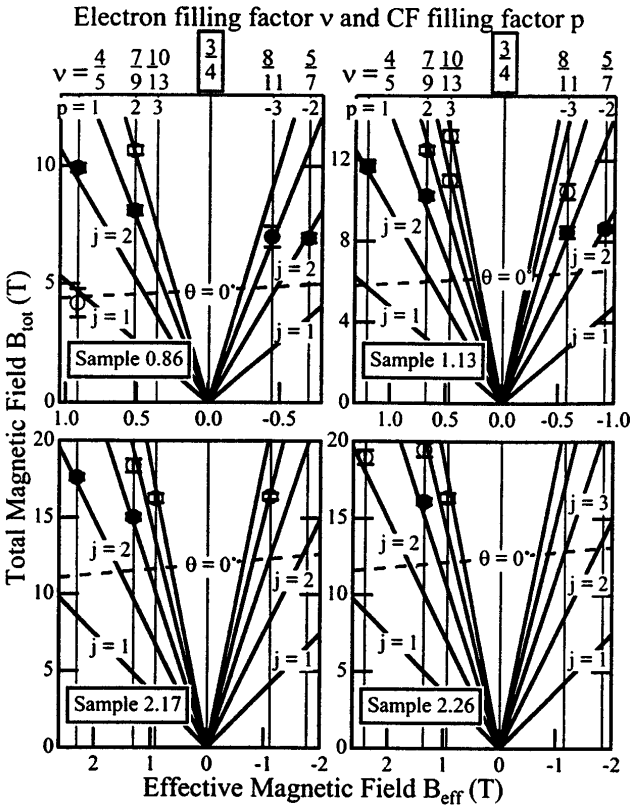


FIG. 3. $B_{\rm tot}$ vs $B_\perp$ for the resistance maxima, such as in Fig. 2, for four samples of very different densities. Filled (open) symbols indicate maxima of greater (less) weight. All data points of all samples reside on fans emanating from the origin using only one fitting parameter, $g^*m^*$, per sample. The regions below the dashed lines correspond to $B_{\rm tot} < B_\perp$ and are inaccessible.

splitting. Solid (open) symbols indicate maxima with greater (less) weight and correspond to maxima with bold (italic) labels in Fig. 2. There exists a diverse set of data points in the $B_{\rm tot}$-$B_{\rm eff}$ plane, all of which can be fitted very well in *all four samples* by a fan of lines whose slopes are exactly in integer ratios, viz. 1:2:3:4:5:6. Only *one fixed* fitting parameter, $g^*m^*$, is used in each fan. Such a constant $g^*m^*$ for many different $j$'s and several $\nu$'s strongly suggests constancy of $g^*$ and $m^*$ separately. The success of this simple procedure in all four specimens establishes the validity of the CF model for four-flux-quanta composite fermions.

Before further evaluating $g^*$ and $m^*$ we digress to the origin of the transport maxima. Our coincidence data reveal level crossings occurring at the Fermi energy as well as level crossings occurring *away from* the Fermi energy. The first are readily understood as a collapse of the gap at $E_f$. The latter have no such simple interpretation, since the gap at $E_f$ remains intact and the coincidence occurs *away* from $E_f$. Around $\nu = 3/2$, both kinds of maxima have been observed and both fall on the same $B_{\rm tot}/B_{\rm eff}$ fan. Around $\nu = 3/4$, on the other hand, *all* observed maxima are from off-$E_f$ crossings. The at-$E_f$ crossings are inaccessible in our specimens, since we can probe only $B_\perp \le B_{\rm tot}$. This highlights the question of the origin of the off-$E_f$ data.

A single-particle CF picture cannot explain these features. A simple model calculation shows that the density of thermally excited CFs is not peaked at off-$E_f$ coincidences, nor can we argue for a sharply increased scattering rate at such coincidences. In fact, if anything, the model indicates the opposite in both cases. Therefore, in order to comprehend the off-$E_f$ resonances, we may have to return to the underlying many-particle picture. There, each CF Landau/spin level represents a different many-particle ground state of different spin and orbital configuration, and a gap separates the ground state from its quasiparticle excitations. At any coincidence, two of the ground states become degenerate, and it seems likely that the gap for quasiparticle excitation would collapse or, at least, experience a strong reduction causing a strong feature in transport. This seems to indicate a limitation of the CF model which needs to be addressed in more depth. However, since around $\nu = 3/2$ off-$E_f$ resonances and at-$E_f$ resonances lie on the same fan, the observed off-$E_f$ resonances around $\nu = 3/4$ are sufficient for our analysis.

We now return to the analysis of $g^*$ and $m^*$. Coincidence measurements determine only the product $g^*m^*$. Traditionally, measurements of the thermal activation energy have provided reliable gap energies $E_g$ which, in the CF picture, can be translated into masses according to $E_g = \hbar e B_{\rm eff}/m^*$ [3]. However, in the present case, at an arbitrary angle, these energy gaps are a mixture of CF Zeeman and CF cyclotron energies. Inspection of the inset of Fig. 2 reveals that for high $B_{\rm tot}$, i.e., high angles, the situation simplifies and the Fermi energy resides between CF Landau levels of the same spin direction. Furthermore, the fit of the coincidence data in Fig. 3 by *one* fan of *fixed* $g^*m^*$ for many *different* $j$'s in each specimen strongly suggests that, within the range of our experiment, the CF $g$ factor does not depend on the CF Landau level. Therefore, a measurement of the energy gap at high tilt angle provides a good measure of $m^*$ without interference from $g^*$.

We have performed several such experiments on the strongest fractions in three specimens. We use the temperature dependence of the Shubnikov–de Haas oscillations in the high-angle limit to determine the mass in the 0.86 sample at $\nu = 4/5$ at five angles and at $\nu = 5/7$ at three angles and in the 1.13 sample at $\nu = 4/5$ at one angle. In the highest density sample, 2.26, we determined the mass at $\nu = 4/5$ at four angles and at $\nu = 5/7$ at three angles (see Table I). We also include the $T$ dependence of neighboring peaks whenever possible. In most cases we have a dynamic range of more than 1 order of magnitude in amplitude. A slight angular dependence of the energy gap is taken into account in our evaluation [8]. The uncertainties reflect the scatter in the data.

TABLE I. Effective masses $m^*$ and effective $g$ factors $g^*$ for CFs with four and two attached flux quanta. $g^*m^*$ is derived from coincidence measurements, $m^*$ is derived from high-angle Shubnikov–de Haas measurements, and $g^*$ is determined by division. Masses are in units of the bare electron mass and $B_\perp$ in units of tesla.

| | $n$ ($10^{11}$ cm$^{-2}$) | $g^*m^*$ | $m^*(\nu = 4/5)$ | $m^*(\nu = 4/5)/\sqrt{B_\perp}$ | $m^*(\nu = 5/7)$ | $m^*(\nu = 5/7)/\sqrt{B_\perp}$ | $g^*$ |
|---|---|---|---|---|---|---|---|
| $^4$CF | 0.86 | 0.39 ± 0.03 | 1.15 ± 0.23 | 0.55 ± 0.11 | 0.58 ± 0.17 | 0.26 ± 0.08 | 0.69 ± 0.21 |
| $^4$CF | 1.13 | 0.42 ± 0.03 | 1.40 ± 0.10 | 0.58 ± 0.04 | | | |
| $^4$CF | 2.17 | 0.54 ± 0.04 | | | | | |
| $^4$CF | 2.26 | 0.54 ± 0.04 | 1.80 ± 0.24 | 0.53 ± 0.07 | 0.90 ± 0.10 | 0.25 ± 0.02 | 0.61 ± 0.08 |
| | | | | | $m^*(\nu = 8/5)$ | $m^*(\nu = 8/5)/\sqrt{B_\perp}$ | |
| $^2$CF | 1.13 | 0.26 ± 0.01 | | | 0.42 ± 0.04 | 0.25 ± 0.02 | 0.60 ± 0.06 |

Clearly the masses of the high-density specimens exceed the masses of the low-density specimens. Such an increase is to be expected since energy gaps scale as $e^2/\ell_0 \propto \sqrt{B_\perp}$, where $\ell_0$ is the magnetic length. This leads to $m^* \propto \sqrt{B_\perp}$, which is a scaling well obeyed by our data, as seen in the "$m^*/\sqrt{B_\perp}$" columns of Table I. It lends strong support to our mass determination.

The mass values derived from the $\nu = 4/5$ features exceed the mass values derived from the $\nu = 5/7$ features by about a factor of 2. From measurements around $\nu = 1/5$, we are aware of drastic resistance variations due to electron localization probably caused by the formation of an electron solid in the filling factor regime [9]. We surmise that the electron-hole symmetric state at $\nu = 4/5$ is similarly affected by hole localization and, therefore, regard only the $\nu = 5/7$ data as being representative of the CF mass around $\nu = 3/4$. Also, as seen in Table I, this $^4$CF mass practically coincides with the $^2$CF mass from the $\nu = 8/5$ FQHE minimum, when scaled by $\sqrt{B_\perp}$. We take this as strong evidence that the mass of $^4$CFs closely resembles the mass of $^2$CFs.

With knowledge of $m^*$, we can derive the values for $g^*$ in the last column of Table I. As it turns out, the values for the $^4$CF $g$ factor are also very similar to the $^2$CF $g$ factor, listed in the last row. The apparent similarity of mass and $g$ factor between $^4$CFs and $^2$CFs represents a remarkable and unforeseen experimental finding. We are not aware of a simple symmetry that would predict such a similarity in properties of different CFs.

In conclusion, we provide first comprehensive data on higher-level composite fermions with four attached flux quanta, $^4$CFs. All experimental results on four samples of different densities can be understood in terms of $^4$CFs having an effective mass $m^*$ and an effective $g$ factor $g^*$. The masses and $g$ factors of $^4$CFs appear very similar to those of $^2$CFs. This is an astounding result, since such a simple relationship between CFs of different levels has neither been foreseen nor is it easily rationalized.

We thank E. Palm and T. Murphy for experimental assistance, and R. R. Du and N. E. Bonesteel for discussions. A portion of this work was performed at the National High Magnetic Field Laboratory which is supported by NSF Cooperative Agreement No. DMR-9527035 and by the State of Florida. D. C. T. and A. S. Y. are supported by NSF and by the DOE.

[1] D. C. Tsui, H. L. Stormer, and A. C. Gossard, Phys. Rev. Lett. **48**, 1559 (1982).

[2] J. K. Jain, Phys. Rev. Lett. **63**, 199 (1989); Phys. Rev. B **40**, 8079 (1989); **41**, 7653 (1990); A. Lopez and E. Fradkin, Phys. Rev. B **44**, 5246 (1991); V. Kalmeyer and S. C. Zhang, Phys. Rev. B **46**, 9889 (1992).

[3] B. I. Halperin, P. A. Lee, and N. Read, Phys. Rev. B **47**, 7312 (1993).

[4] R. L. Willett, R. R. Ruel, K. W. West, and L. N. Pfeiffer, Phys. Rev. Lett. **71**, 3846 (1993); W. Kang, H. L. Stormer, L. N. Pfeiffer, K. W. Baldwin, and K. W. West, Phys. Rev. Lett. **71**, 3850 (1993); V. J. Goldman, B. Su, and J. K. Jain, Phys. Rev. Lett. **72**, 2065 (1994); J. H. Smet, D. Weiss, R. H. Blick, G. Lutjering, K. von Klitzing, R. Fleischmann, R. Ketzmerick, T. Geisel, and G. Weimann, Phys. Rev. Lett. **77**, 2272 (1996).

[5] R. R. Du, H. L. Stormer, D. C. Tsui, L. N. Pfeiffer, and K. W. West, Phys. Rev. Lett. **70**, 2944 (1993); D. R. Leadley, R. J. Nicholas, C. T. Foxon, and J. J. Harris, Phys. Rev. Lett. **72**, 1906 (1994); H. C. Manoharan, M. Shayegan, and S. J. Klepper, Phys. Rev. Lett. **73**, 3270 (1994); P. T. Coleridge, Z. W. Wasilewski, P. Zawadzki, A. S. Sachrajda, and H. A. Carmona, Phys. Rev. B **52**, 11 603 (1995).

[6] J. P. Eisenstein, H. L. Stormer, L. N. Pfeiffer, and K. W. West, Phys. Rev. Lett. **62**, 1540 (1989); R. G. Clark, S. R. Haynes, A. M. Suckling, J. R. Mallett, P. A. Wright, J. J. Harris, and C. T. Foxon, Phys. Rev. Lett. **62**, 1536 (1989); J. E. Furneaux, D. A. Syphers, and A. G. Swanson, Phys. Rev. Lett. **63**, 1098 (1989); A. Sachrajda, R. Boulet, Z. Wasilewski, P. Coleridge, and F. Guillon, Solid State Commun. **74**, 1021 (1990); L. W. Engel, S. W. Hwang, T. Sajoto, D. C. Tsui, and M. Shayegan, Phys. Rev. B **45**, 3418 (1992).

[7] R. R. Du, A. S. Yeh, H. L. Stormer, D. C. Tsui, L. N. Pfeiffer, and K. W. West, Phys. Rev. Lett. **75**, 3926 (1995).

[8] P. J. Gee, F. M. Peters, J. Singleton, S. Uji, H. Aoki, C. T. B. Foxon, and J. J. Harris, Phys. Rev. B **54**, R14 313 (1996).

[9] H.-W. Jiang, R. L. Willett, H. L. Stormer, D. C. Tsui, L. N. Pfeiffer, and K. W. West, Phys. Rev. Lett. **65**, 633 (1990).